Norman Fitz-Coy
Department of Aerospace Engineering, Mechanics, and Engineering Science
University of Florida
Gainesville, FL 32611-6250

Analysis of Multiaxis Vibration Simulators

A mathematical procedure that quantitatively addresses issues critical to the design and operation of multiaxis vibration simulators is presented. Both kinematic and dynamic issues are considered. The analysis is applied to both 3 and 6 degrees of freedom configurations. The existence of singular configurations is mentioned and appropriate corrective measures are recommended. A methodology for determining the required actuator commands is also presented. © *1995 John Wiley & Sons, Inc.*

INTRODUCTION

Due to the increasing complexity of new equipment, vibration test specifications are changing. Currently, there is a shift away from the "boiler plate" testing of the past toward a "customer defined" testing procedure. This trend, along with these new specifications will require that vibration test facilities become more versatile; that is, test facilities will be required to perform *true* multiaxis vibration testing. By utilizing multiaxis vibration testing facilities, the synergistic effects of simultaneously exciting *all* modes can be included, thus making customer defined tests more realistic.

The idea of multiaxis vibration testing is not entirely new (Merklinghaus, 1977; Hahn and Raasch, 1986); it has been inexistence for some time in the seismic community (high frequency, >1 kHz) and in the automotive and aerospace communities (low frequency, ~2–100 Hz). The success of multiaxis vibration simulators in the midfrequency range (100–500 Hz) has been limited to date.

Existing multiaxis vibration simulators are, to some extent, based on the Stewart platform design. In principle, the Stewart platform describes any two-body mechanism utilizing parallel connections (Stewart, 1965; Fitcher, 1986). Typically, in these mechanisms, the direction of actuation is not fixed in some "inertial" frame of reference. For low frequency applications, there are numerous actuation systems that can provide variable direction actuation (e.g., screw jacks, hydraulic cylinders, etc.); thus, the Stewart platform is well suited for motion simulators and low frequency vibration simulators. However, for systems in the midfrequency range with large load capacities, electrohydraulic exciters are almost always required. In the current state of the art, these exciters operate more efficiently when anchored to reaction masses, resulting in fixed actuation direction. Thus, one of the primary difficulties associated with the design and utilization of large capacity, midfrequency vibration simulators is the kinematic constraints imposed by existing hardware.

In this article, the kinematic and dynamic issues associated with the design and utilization of large capacity, midfrequency range, multiaxis vibration simulators are addressed.

Received November 15, 1993; Accepted June 18, 1995.
Shock and Vibration, Vol. 2, No. 6, pp. 461–470 (1995)

CCC 1070-9622/95/060461-10

KINEMATIC CONSIDERATIONS

In the following text, it is assumed that the multiaxis vibration simulator has a rigid platform. Thus, discussions on vibrational degrees of freedom (DOF) are actually discussions of the 6 DOF of the platform, those being the three translations of the center of mass (c.m.) and the three rotations about the c.m. It is also assumed that there are no redundant actuators; that is, there are r actuators ($r \leq 6$) capable of imparting r vibrational DOF to the simulator. Each actuator has one end attached to the platform and the other attached to the base [see Fig. 1(a)].

Dextral, orthogonal, body fixed coordinate frames $\mathcal{F}_P$ and $\mathcal{F}_B$ are defined in the platform and the base, respectively [see Fig. 1(b)]. It is convenient (see Dynamic Considerations) to locate the origin of $\mathcal{F}_P$ at the c.m., C, of the platform; the origin, O, of $\mathcal{F}_B$ can be arbitrarily located. Let P_i denote the attachment point of the ith actuator in the platform and B_i the attachment point of the same actuator in the base.

The following notation is adopted: $\mathbf{a}$ denotes a vector while ${}^A\mathbf{a}$ denotes a column matrix whose elements are the components of $\mathbf{a}$ coordinatized in $\mathcal{F}_A$; $\mathbf{L}_{PB}$ denotes the orientation of the $\mathcal{F}_P$ relative to $\mathcal{F}_B$. [*Note*: $\mathbf{L}_{PB}$ will also be used as the transformation matrix from $\mathcal{F}_B$ to $\mathcal{F}_P$ that implies $\mathbf{L}_{BP}$ $(=\mathbf{L}_{PB}^{-1})$ represents the inverse transformation].

The force exerted by the ith actuator can be expressed as

$$\mathbf{F}_i = f_i \hat{\mathbf{u}}_i, \tag{1}$$

where $\hat{\mathbf{u}}_i$ is a unit vector in the direction of the line of action (LOA) of the force and f_i is the magnitude of the force. The LOA, and hence $\hat{\mathbf{u}}_i$, are referred to as line coordinates (Fitcher, 1986; Hunt, 1978). The unit LOA vector is [see Fig. 1(b)]

$$\hat{\mathbf{u}}_i = (\mathbf{r}_i^P - \mathbf{r}_i^B - \mathbf{R})/\sigma_i \tag{2}$$

where $\mathbf{r}_i^P$ and $\mathbf{r}_i^B$ are the position vectors of P_i and B_i, respectively. $\mathbf{R}$ specifies the location of the origin of $\mathcal{F}_B$ relative to the origin of $\mathcal{F}_P$ and σ_i is the magnitude of the LOA vector. Coordinatizing the unit LOA vector in $\mathcal{F}_B$ results in

$${}^B\hat{\mathbf{u}}_i = \frac{1}{\sigma_i}(\mathbf{L}_{BP}{}^P\mathbf{r}_i^P - {}^B\mathbf{r}_i^B - {}^B\mathbf{R}) \tag{3}$$

where ${}^P\mathbf{r}_i^P = [x_i^P \quad y_i^P \quad z_i^P]^T$, ${}^B\mathbf{r}_i^B = [x_i^B \quad y_i^B \quad z_i^B]^T$, and ${}^B\mathbf{R} = [X \quad Y \quad Z]^T$.

In general, P_i does not coincide with the c.m. of the platform. Thus, each actuator's force, $\mathbf{F}_i$, generates a moment about the platform's c.m. given by

$$\mathbf{M}_i = \mathbf{r}_i^P \times \mathbf{F}_i = (\mathbf{r}_i^P \times \hat{\mathbf{u}}_i) f_i = \mathbf{m}_i^P f_i. \tag{4}$$

$\mathbf{m}_i^P$ is referred to as the moment arm of f_i and is a vector normal to the plane formed by $\mathbf{r}_i^P$ and $\hat{\mathbf{u}}_i$ (i.e., the plane containing the origin and the LOA of the ith force). The magnitude of $\mathbf{m}_i^P$ represents the shortest distance from the LOA vector to the platform's c.m. Because $\mathbf{M}_i$ represents a moment about the platform's c.m., it is convenient to coordinatize this quantity in $\mathcal{F}_P$. Thus,

$${}^P\mathbf{M}_i = {}^P\mathbf{m}_i^P f_i, \tag{5}$$

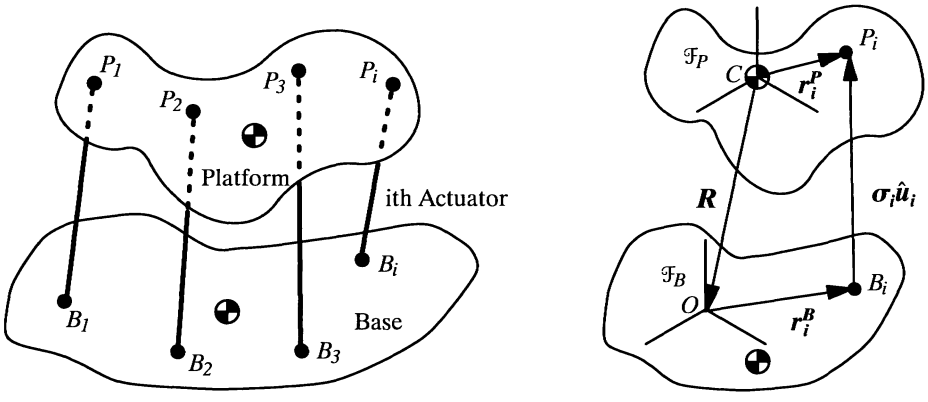

FIGURE 1 Generalized multiaxis simulator.

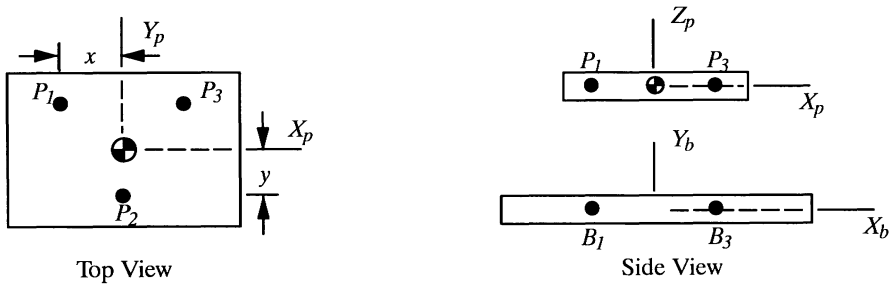

FIGURE 2 Typical actuator layout in 3-DOF simulators.

where ${}^P\mathbf{m}_i^P = {}^P\tilde{\mathbf{r}}_i^P \, {}^P\hat{\mathbf{u}}_i$; ${}^P\tilde{\mathbf{r}}_i^P$ is the skew-symmetric matrix

$$\begin{bmatrix} 0 & -z_i^P & y_i^P \\ z_i^P & 0 & -x_i^P \\ -y_i^P & x_i^P & 0 \end{bmatrix}$$

and ${}^P\hat{\mathbf{u}}_i = \mathbf{L}_{PB} {}^B\hat{\mathbf{u}}_i$.

A 3-DOF Example

Consider the case where $r = 3$. Figure 2 depicts a typical layout of the actuators. The actuators are so placed that the resulting motions of the platform are z translation (as seen from $\mathcal{F}_B$), roll and pitch (Fitz–Coy and Chatterjee, 1994). The actuators can be coupled to the platform in two ways—one results in a fixed LOA [Fig. 3(a)] and the other results in a variable LOA [Fig. 3(b)]. In both cases, the LOAs of the actuators output are fixed in $\mathcal{F}_B$; however, the LOA of the force transmitted to the platform is dependent on the coupling used. It is this transmitted force that we are concerned with and we will refer to its LOA as the LOA of the actuator.

Consider the coupling concept depicted in Fig. 3(a). In this case, ${}^B\hat{\mathbf{u}}_i = [0 \quad 0 \quad 1]^T$. Now, let us assume the simulator is executing a pitching motion through an angle θ, then

$$\mathbf{L}_{BP} = \begin{bmatrix} \cos\theta & 0 & \sin\theta \\ 0 & 1 & 0 \\ -\sin\theta & 0 & \cos\theta \end{bmatrix}$$

and Eq. (3) becomes

$${}^B\hat{\mathbf{u}}_i = \frac{1}{\sigma_i} \begin{bmatrix} x_i^P \cos\theta + z_i^P \sin\theta - x_i^B - X \\ y_i^P - y_i^B - Y \\ -x_i^P \sin\theta + z_i^B \cos\theta - z_i^B - Z \end{bmatrix}. \tag{6}$$

Because the location of the origin of $\mathcal{F}_B$ is arbitrary, it can be chosen such that $X = Y = 0$ (i.e., the reference points are vertically aligned as seen from $\mathcal{F}_B$). Also, in most instances, the actuator attach points are in the xy plane of the respective coordinate frame (i.e., $z_i^P = z_i^B = 0$). Under these conditions, Eq. (6) becomes

$${}^B\hat{\mathbf{u}}_i = \frac{1}{\sigma_i} \begin{bmatrix} x_i^P \cos\theta - x_i^B \\ y_i^P - y_i^B \\ -x_i^P \sin\theta - Z \end{bmatrix}.$$

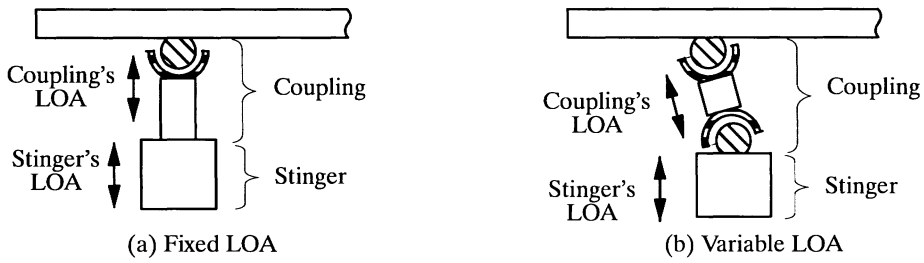

FIGURE 3 Typical actuator attachment.

The condition necessary for ${}^B\hat{\mathbf{u}}_i = [0 \quad 0 \quad 1]^T$ are

$$x_i^P \cos\theta - x_i^B = 0 \quad \text{and} \quad y_i^P - y_i^B = 0.$$

The second requirement is easily satisfied by allowing vertical alignment of these points in the reference state. However, the first requirement implies that both P_i and B_i cannot be fixed points in their respective bodies. In fact, if we assume that P_i is fixed in the platform, then B_i must be allowed to move in the X_b direction. For the layout depicted in Fig. 2, motion in the X_b direction is required for actuators 1 and 3; actuator 2 requires no motion in the X_b direction because $x_i^P = x_i^B \equiv 0$. In a similar manner, if we assume that the platform is executing rolling motion, it can be shown that motion in the Y_b direction must be allowed for either P_i or B_i. Thus, fixed LOA actuation requires movable actuator attachment points. An example of this coupling concept can be found at the RTTC Dynamic test facility at Huntsville.

The need for movable actuator attachment points can be eliminated using the coupling concept depicted in Fig. 3(b). However, it will be shown in the following section that this concept is singular unless other constraints are provided.

DYNAMIC CONSIDERATIONS

It is often necessary to determine the forces and moments that the actuators must provide to obtain the desired vibrations. In this section, a procedure that allows the computation of actuator commands is developed. Although screw theory could be used to develop the procedure, the authors see no reason to use this approach rather than the Newton–Euler approach (upon which the screw theory is based).

A free body diagram of the system is shown in Fig. 4. There are r actuator forces, $\mathbf{F}_1$, $\mathbf{F}_2, \ldots, \mathbf{F}_r$, a weight force, $\mathbf{W}$, and an external force $\mathbf{F}_E$ (which includes all other forces) acting on the system. Application of Newton's second law of motion provides

$$\frac{d}{dt}(m\mathbf{V}_c^P) = m\mathbf{a}_c^P = \mathbf{F}_1 + \mathbf{F}_2 + \cdots + \mathbf{F}_r + \mathbf{W} + \mathbf{F}_E. \tag{7}$$

It is convenient to coordinatize Eq. (7) in $\mathcal{F}_B$ because the translational motions of interest are best described in $\mathcal{F}_B$. Coordinatizing and rearranging Eq. (7) yields

$${}^B\mathbf{F}_1 + {}^B\mathbf{F}_2 + \cdots + {}^B\mathbf{F}_r = m({}^B\mathbf{a}_c^P - {}^B\mathbf{g}) - {}^B\mathbf{F}_E, \tag{8}$$

where ${}^B\mathbf{W}$ is replaced with $m{}^B\mathbf{g}$. Utilizing Eqs. (1) and (3), the actuator forces can be expressed as ${}^B\mathbf{F}_i = {}^B\hat{\mathbf{u}}_i f_i$ that allows Eq. (8) to be rewritten as

$$[{}^B\hat{\mathbf{u}}_1 \quad {}^B\hat{\mathbf{u}}_2 \quad \cdots \quad {}^B\hat{\mathbf{u}}_r] \begin{bmatrix} f_1 \\ f_2 \\ \vdots \\ f_r \end{bmatrix} = m({}^B\mathbf{a}_c^P - {}^B\mathbf{g}) - {}^B\mathbf{F}_E. \tag{9}$$

The rotational motion is governed by Euler's equations (Goldstein, 1980). When applied about the c.m. of a body, Euler's equations take the simple form shown in Eq. (10)—hence, the motivation for the choice of origin of $\mathcal{F}_P$.

$$\frac{d}{dt}(\mathbf{H}_c^P) = \mathbf{M}_1 + \mathbf{M}_2 + \cdots + \mathbf{M}_r + \mathbf{M}_E, \tag{10}$$

where $\mathbf{H}_c^P = \mathbf{I}_c^P \cdot \boldsymbol{\omega}^P$ is the angular momentum of the platform about its c.m. $\mathbf{I}_c^P$ is the platform's centroidal inertia dyadic and $\boldsymbol{\omega}^P$ is the angular velocity of the platform. The weight force acts through the c.m. and therefore produces no moment about that point. Because we are interested in the attitude of $\mathcal{F}_P$ with respect to $\mathcal{F}_B$, it is convenient to coordinatize Eq. (10) in $\mathcal{F}_P$. Substituting the expression for angular momentum into Eq. (10) and coordinatizing the resulting expression in $\mathcal{F}_P$, yields

$${}^P\mathbf{M}_1 + {}^P\mathbf{M}_2 + \cdots + {}^P\mathbf{M}_r = {}^P\mathbf{I}_c^{PP}\dot{\boldsymbol{\omega}} + {}^P\tilde{\boldsymbol{\omega}}{}^P\mathbf{I}_c^{PP}\boldsymbol{\omega} - {}^P\mathbf{M}_E. \tag{11}$$

Via Eq. (5), Eq. (11) can be rewritten as

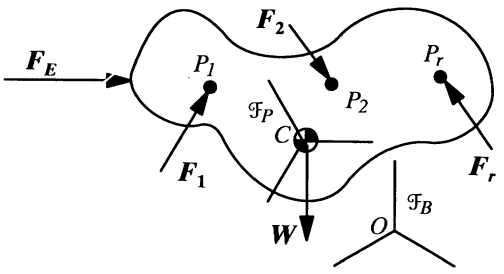

FIGURE 4 Free body diagram of platform.

$$[{}^P\mathbf{m}_1^P \quad {}^P\mathbf{m}_2^P \quad \cdots \quad {}^P\mathbf{m}_r^P]\begin{bmatrix} f_1 \\ f_2 \\ \vdots \\ f_r \end{bmatrix} = {}^P\mathbf{I}_c^{PP}\dot{\omega} + {}^P\tilde{\omega}{}^P\mathbf{I}_c^{PP}\omega - {}^P\mathbf{M}_E. \tag{12}$$

Combining Eqs. (9) and (12) yields

$$\begin{bmatrix} {}^B\mathbf{u}_1 & {}^B\mathbf{u}_2 & \cdots & {}^B\mathbf{u}_r \\ {}^P\mathbf{m}_1^P & {}^P\mathbf{m}_2^P & \cdots & {}^P\mathbf{m}_r^P \end{bmatrix}\begin{bmatrix} f_1 \\ f_2 \\ \vdots \\ f_r \end{bmatrix} = \begin{bmatrix} m({}^B\mathbf{a}_c^P - {}^B\mathbf{g}) - {}^B\mathbf{F}_E \\ {}^P\mathbf{I}_c^{PP}\dot{\omega} + {}^P\tilde{\omega}{}^P\mathbf{I}_c^{PP}\omega - {}^P\mathbf{M}_E \end{bmatrix}. \tag{13}$$

Equation (13) is of the form

$$\underset{(6\times r)}{\mathcal{P}} \quad \underset{(r\times 1)}{\{f\}} = \underset{(6\times 1)}{\{\mathcal{C}\}} \tag{14}$$

where $\mathcal{P}$ is a matrix of line coordinates and moment arms; it is referred to in the literature as the matrix of Plucker coordinates (Fitcher, 1986; Hunt, 1978). The ith element of $\{f\}$ represents the level of actuation of the ith actuator. The ith element of $\{\mathcal{C}\}$ is the difference of the ith generalized inertia force and the ith generalized external force; in most instances, the ith generalized external force will be zero.

Equation (14) can be interpreted in the following manner: given the desired generalized accelerations (hence, the generalized force matrix $\{\mathcal{C}\}$), determine the actuator commands $\{f\}$ required to generate these accelerations. Before determining the desired actuator commands, we digress for a moment to prove using the singular value decomposition (SVD) (Golub and Van Loan, 1989), that r actuators have, at most, control authority over r DOF (i.e., r actuators can at best excite r DOF in a controllable manner).

Via the SVD, $\mathcal{P}$ can be represented as $\mathcal{P} = \mathbf{U}\Sigma\mathbf{V}^T$, where $\mathbf{U}$ and $\mathbf{V}$ are, respectively, (6×6) and $(r \times r)$ unitary matrices. Assuming that $\mathcal{P}$ has full column rank (i.e., there are no redundant actuators), then Σ is a $(6 \times r)$ matrix of the form

$$\Sigma = \begin{bmatrix} \operatorname{diag}(\sigma_1, \ldots, \sigma_r) \\ \hline 0 \end{bmatrix} \begin{matrix} \}r \\ \}6-r \end{matrix}.$$

Substituting $\mathcal{P} = \mathbf{U}\Sigma\mathbf{V}^T$ into Eq. (14) and premultiplying both sides by $\mathbf{U}^T$ yields

$$\Sigma\mathbf{V}^T\{f\} = \mathbf{U}^T\{\mathcal{C}\}. \tag{15}$$

From the definition of Σ, the lower $(6 - r)$ rows of Eq. (15) must be zero. Therefore, only r DOF are controllable with r actuators. For the case involving redundant actuators, the above also holds true except that the rank $(\mathcal{P}) = p < r$. Thus, in this case, only p DOF are controllable with r actuators. Although the discussion presented here is specific to the case of $r \leq 6$, the analysis can easily be extended to include cases of $r > 6$.

This completes the proof. We now return to the determination of the actuator commands. Two cases are considered: first, the fixed LOA depicted in Fig. 3(a), followed by the variable LOA depicted in Fig. 3(b).

Case 1: $r = 3$, Fixed LOA

Consider the 3-DOF layout shown in Fig. 2. For this case, the LOAs are given by ${}^B\hat{\mathbf{u}}_i = [0 \quad 0 \quad 1]^T$, $i = 1, 2, 3$. The actuator locations in the platform are ${}^P\mathbf{r}_1^P = [-x \quad y \quad 0]^T$, ${}^P\mathbf{r}_2^P = [0 \quad -y \quad 0]^T$, and ${}^P\mathbf{r}_3^P = [x \quad y \quad 0]^T$.

The platform is assumed to execute small angular displacements (i.e., $\leq 10°$) through angles ϕ, θ, ψ that are, respectively, the roll, pitch, and yaw of the platform. This assumption is not mandatory for the analysis; however, the resulting expressions are greatly simplified with its adaptation. Also, a requirement of small angular motion is not restrictive for vibration simulators.

The small angle transformation matrix is

$$\mathbf{L}_{PB} = \begin{bmatrix} 1 & \psi & -\theta \\ -\psi & 1 & \phi \\ \theta & -\phi & 1 \end{bmatrix}.$$

The moment arm of each actuator, ${}^P\mathbf{m}_i^P$, is determined from Eq. (5). For actuator 1, this becomes

$${}^P\mathbf{m}_1^P = \begin{bmatrix} 0 & 0 & y \\ 0 & 0 & x \\ -y & -x & 0 \end{bmatrix}\begin{bmatrix} 1 & \psi & -\theta \\ -\psi & 1 & \phi \\ \theta & -\phi & 1 \end{bmatrix}\begin{bmatrix} 0 \\ 0 \\ 1 \end{bmatrix} = \begin{bmatrix} y \\ x \\ \theta y - \phi x \end{bmatrix}.$$

${}^P\mathbf{m}_2^P = [-y \quad 0 \quad -\theta y]^T$ and ${}^P\mathbf{m}_3^P = [y \quad -x \quad (\theta y + \phi x)]^T$ are obtained in a similar manner. The matrix of Plucker coordinates [Eq. (13)] can now be assembled.

$$\mathcal{P} = \begin{bmatrix} 0 & 0 & 0 \\ 0 & 0 & 0 \\ 1 & 1 & 1 \\ y & -y & y \\ x & 0 & -x \\ \theta y - \phi x & -\theta y & \theta y + \phi x \end{bmatrix}.$$

Assuming no actuator redundancy, it was shown above that the maximum number of controllable DOF is three. Thus, we need only consider (3 × 3) partitions of $\mathcal{P}$, in which case, Eq. (14) becomes

$$\begin{bmatrix} \mathcal{P}_\mathbf{U} \\ \mathcal{P}_L \end{bmatrix} \{f\} = \begin{bmatrix} \mathcal{C}_\mathbf{U} \\ \mathcal{R} \end{bmatrix}. \tag{16}$$

The upper partition results in $\mathcal{P}_\mathbf{U}\{f\} = \{\mathcal{C}_\mathbf{U}\}$, from which $\{f\}$ is determined; this implies that $\mathcal{P}_\mathbf{U}$ must be nonsingular to uniquely specify the force. The lower partition gives $\mathcal{P}_L\{F\} = \{\mathcal{R}\}$, where $\mathcal{R}$ indicates residual motion in the remaining three DOF. Ideally, $\mathcal{R}$ should be zero.

The following partition of $\mathcal{P}$ results from considering the x, y, and z translations of the c.m. of the platform.

$$\mathcal{P}_\mathbf{U} = \begin{bmatrix} 0 & 0 & 0 \\ 0 & 0 & 0 \\ 1 & 1 & 1 \end{bmatrix}.$$

In this case, $\mathcal{P}_\mathbf{U}$ is singular, that implies that it is impossible to excite in a controllable manner the three translational DOF using three vertical LOA actuators. [*Note*: this is actually a case of actuator redundancy because rank $(\mathcal{P}_\mathbf{U}) = 1$.] Similarly, it can be shown that it is impossible to controllably excite the combination of three rotational DOF or any other combinations of three DOF involving either x or y translations.

Consider now the combination involving z translation, roll, and pitch. In this case,

$$\mathcal{P}_\mathbf{U} = \begin{bmatrix} 1 & 1 & 1 \\ y & -y & y \\ x & 0 & -x \end{bmatrix} \quad \text{and} \quad \mathcal{P}_L = \begin{bmatrix} 0 & 0 & 0 \\ 0 & 0 & 0 \\ \theta y - \phi x & -\theta y & \theta y + \phi x \end{bmatrix}.$$

The desired actuation levels are obtained from

$$\{f = \mathcal{P}_\mathbf{U}^{-1}\{\mathcal{C}_\mathbf{U}\} = \frac{1}{\Delta}\begin{bmatrix} xy & x & 2y \\ 2xy & -2x & 0 \\ xy & x & -2y \end{bmatrix}\{\mathcal{C}_\mathbf{U}\},$$

where $\Delta = 4xy \neq 0$. Excitation in the z direction can be represented illustratively by $\mathcal{C}_\mathbf{U}\} = [1 \quad 0 \quad 0]^T$, which implies the amplitudes of the actuation commands be in the following ratio: $\{f\} = [1 \quad 2 \quad 1]^T$. Computation of the lower partition provides $\mathcal{R} \equiv 0$, implying that motion exists only in the desired direction. Similar results can be obtained for roll and pitch motions. Excitation about the roll axis and the pitch axis is represented by $\{\mathcal{C}_\mathbf{U}\} = [0 \quad 1 \quad 0]^T$ and $\{\mathcal{C}_\mathbf{U}\} = [0 \quad 0 \quad 1]^T$, respectively.

Case 2: $r = 3$, Variable LOA

The results of the previous section are not entirely surprising. The more interesting case involves application of the procedure to the variable LOA configuration. Consider again the 3-DOF layout shown in Fig. 2. To develop the variable LOA approach, variables α_i and β_i that represent the roll and pitch, respectively, of the ith actuator's LOA (see Fig. 5) are introduced. These quantities are defined as:

$$\alpha_1 = -\frac{\Delta y - \psi x}{l}, \quad \alpha_2 = -\frac{\Delta y}{l}, \quad \alpha_3 = -\frac{\Delta y + \psi x}{l},$$

$$\beta_1 = \beta_3 = \frac{\Delta x - \psi y}{l}, \quad \beta_2 = \frac{\Delta x + \psi y}{l}.$$

In $\mathcal{F}_B$, the unit LOA vector of the ith actuator is

$${}^B\hat{\mathbf{u}}_i = \begin{bmatrix} 1 & 0 & \beta_i \\ 0 & 1 & -\alpha_i \\ -\beta_i & \alpha_i & 1 \end{bmatrix}\begin{bmatrix} 0 \\ 0 \\ 1 \end{bmatrix} = \begin{bmatrix} \beta_i \\ -\alpha_i \\ 1 \end{bmatrix}.$$

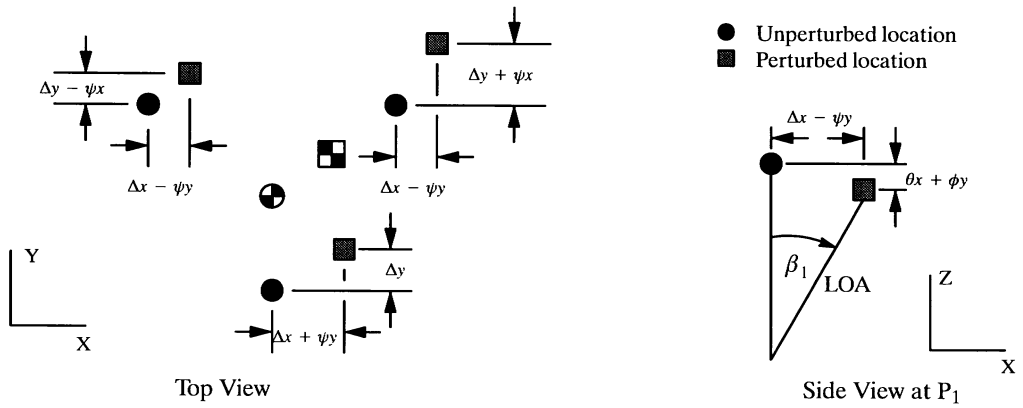

FIGURE 5 Relative displacements of actuator attachment points resulting from arbitrary platform motions.

Having determined ${}^{B}\hat{\mathbf{u}}_i$, the matrix of Plucker coordinates is developed as outlined in the previous section.

$$\mathcal{P} = \begin{bmatrix} \beta_1 & \beta_2 & \beta_3 \\ -\alpha_1 & -\alpha_2 & -\alpha_3 \\ 1 & 1 & 1 \\ y & -y & y \\ x & 0 & -x \\ y(\theta-\beta_1) - x(\phi-\alpha_1) & -y(\theta-\beta_2) & y(\theta-\beta_3) + x(\phi-\alpha_3) \end{bmatrix}$$

Observe that, if $\alpha_i = \beta_i = 0$, then the fixed LOA case is recovered.

As before, we are limited to the controllable excitation of 3 DOF. Consider the case of three translational DOF. For this case, $\mathcal{P}_U$ is

$$\mathcal{P}_U = \begin{bmatrix} \beta_1 & \beta_2 & \beta_3 \\ -\alpha_1 & -\alpha_2 & -\alpha_3 \\ 1 & 1 & 1 \end{bmatrix}$$

In general, $\mathcal{P}_U$ is nonsingular because $\Delta = \beta_1(\alpha_3 - \alpha_2) + \beta_2(\alpha_1 - \alpha_3) + \beta_3(\alpha_2 - \alpha_1) \neq 0$, provided that $\alpha_i, \beta_i \neq 0$, $\forall i$. Therefore, unique actuator commands exist that are capable of producing excitation in the three translational DOF. In a similar manner, other combinations of 3 DOF could be considered, each resulting in a nonsingular $\mathcal{P}_U$ implying that unique actuator commands exist for these DOF combinations. However, in each case, the lower partition, $\mathcal{P}_L\{f\} = \{\mathcal{R}\}$, results in a nonzero residual in the remaining DOF. For example, in the case of the three translational DOF combination executing x translation,

$$\mathcal{P}_L\{f\} = \begin{bmatrix} y & -y & y \\ x & 0 & -x \\ y(\theta-\beta_1) - x(\phi-\alpha_1) & -y(\theta-\beta_2) & y(\theta-\beta_3) + x(\phi-\alpha_3) \end{bmatrix} \begin{bmatrix} \alpha_3 - \alpha_2 \\ \alpha_1 - \alpha_3 \\ \alpha_2 - \alpha_1 \end{bmatrix} \neq 0.$$

Thus, it is impossible to uniquely excite only three DOF. This configuration is said to be singular because all 6 DOF are excitable with three exciters.

It was previously noted (see Kinematic Considerations) that this configuration is singular unless constraints were provided. Now consider that the yaw rotation of the platform is constrained, then

$$\alpha_1 = \alpha_2 = \alpha_3 = -\frac{\Delta y}{l}, \quad \text{and} \quad \beta_1 = \beta_2\beta_3 = \frac{\Delta x}{l}.$$

In this case, it can be shown that $\mathcal{P}_U$ is singular for all 3-DOF combinations except the combination involving z translation, roll, and pitch. Computation of $\mathcal{R}$ shows additional motions in the x and y directions (which were not constrained) and no motion in yaw (which was constrained!). Therefore, to obtain only the desired 3 DOF, the c.m. must also be constrained in the x and y directions.

Case 3: $r = 6$, Variable LOA

Consider the 6-DOF system shown in Fig. 6. The contributions of the three vertical actuators to $\mathcal{P}$ remain unchanged. The contributions of the horizontal actuators are determined in a manner similar to the variable LOA case discussed above. Again, it is necessary to define roll (ν_i), pitch (λ_i), and yaw (γ_i) attitudes for the LOA of the ith horizontal actuator. These quantities are:

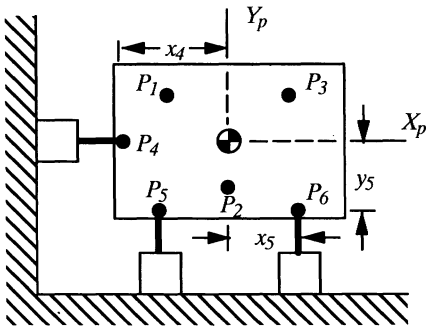

FIGURE 6 A 6-DOF simulator.

$$\nu_4 = 0, \quad \nu_5 = \frac{\Delta z + \theta x_5 - \phi y_5}{l} - \frac{\Delta x^2 + \Delta y^2}{2l^2},$$

$$\nu_6 = \frac{\Delta z - \theta x_5 - \phi y_5}{l} - \frac{\Delta x^2 + \Delta y^2}{2l^2},$$

$$\lambda_4 = -\frac{\Delta z - \theta x_4}{l} + \frac{\Delta x^2 + \Delta y^2}{2l^2}, \quad \lambda_5 = \lambda_6 = 0,$$

$$\gamma_4 = \frac{\Delta y - \psi x_4}{l} - \frac{\Delta x^2 + \Delta z^2}{2l^2},$$

$$\gamma_5 = \gamma_6 = \frac{\Delta x + \psi(x_5 + y_5)}{l} + \frac{\Delta y^2 + \Delta z^2}{2l^2}.$$

Similar to the procedure of the previous section, the matrix of Plucker coordinates is constructed.

$$\mathcal{P} = \begin{bmatrix} \beta_1 & \beta_2 & \beta_3 \\ -\alpha_1 & -\alpha_2 & -\alpha_3 \\ 1 & 1 & 1 \\ y & -y & y \\ x & 0 & -x \\ [y(\theta - \beta_1) - x(\phi - \alpha_1)] & [-y(\theta - \beta_2)] & [y(\theta - \beta_3) + x(\phi - \alpha_3)] \end{bmatrix}$$

$$\begin{bmatrix} 1 & -\gamma_5 & -\gamma_6 \\ \gamma_4 & 1 & 1 \\ -\lambda_4 & \nu_5 & \nu_6 \\ 0 & -y_5(\nu_5 - \phi) & -y_5(\nu_6 - \phi) \\ [x_4(-\lambda_4 + \theta)] & [x_5(\nu_5 - \phi)] & [-x_5(\nu_6 - \phi)] \\ [-x_4(\gamma_4 + \psi)] & [y_5(-\nu_5 + \psi) - x_5] & [y_5(-\nu_6 + \psi) + x_5] \end{bmatrix}$$

Although not obvious, it can be shown that $\mathcal{P}$ is nonsingular. Therefore, the variable LOA 6-DOF configuration can controllably simulate six vibrational DOF. It is important to notice that this is accomplished without the need for additional constraints, as was required with the 3-DOF configuration.

For illustrative purposes, consider an initial configuration in which all the LOAs are unperturbed, (i.e., $\alpha_i = \beta_i = \nu_1 = \lambda_i = \gamma_i = 0$), then

$$\mathcal{P}(t_0) = \begin{bmatrix} 0 & 0 & 0 & 1 & 0 & 0 \\ 0 & 0 & 0 & 0 & 1 & 1 \\ 1 & 1 & 1 & 0 & 0 & 0 \\ y & -y & y & 0 & 0 & 0 \\ x & 0 & -x & 0 & 0 & 0 \\ 0 & 0 & 0 & 0 & -x_5 & x_5 \end{bmatrix} \quad \text{and} \quad \mathcal{P}^{-1}(t_0) = \begin{bmatrix} 0 & 0 & \frac{1}{4} & \frac{1}{4y} & \frac{1}{2x} & 0 \\ 0 & 0 & \frac{1}{2} & -\frac{1}{2y} & 0 & 0 \\ 0 & 0 & \frac{1}{4} & \frac{1}{4y} & -\frac{1}{2x} & 0 \\ 1 & 0 & 0 & 0 & 0 & 0 \\ 0 & \frac{1}{2} & 0 & 0 & 0 & -\frac{1}{2x_5} \\ 0 & \frac{1}{2} & 0 & 0 & 0 & \frac{1}{2x_5} \end{bmatrix}.$$

Illustratively, vibrations in the x direction are represented by $\{\mathcal{C}\} = [1 \ 0 \ 0 \ 0 \ 0 \ 0 \ 0]^T$. From Eq. (14), $\{f\}(t_0) = [0 \ 0 \ 0 \ 1 \ 0 \ 0 \ 0]^T$, which implies excitation of actuator 4. However, excitation of only actuator 4 results in all other DOF, except roll motion, being excited. This is demonstrated by postmultiplying $\mathcal{P}$ by $\{f\}(t_0)$. Similar results can be obtained for any other desired motion. These results reinforce the fact that kinematic and dynamic coupling exists in multi-DOF systems. Notice that the kinematic couplings (i.e., α_i, β_i, ν_i, λ_i, γ_i) are inversely proportional to the length of the device that couples the actuator to the platform; therefore, by increasing the lengths of these devices, the kinematic coupling can be reduced, but *cannot* be eliminated. The dynamic coupling is a function of the geometry of the platform/payload combination and therefore it is not always possible to minimize the effects of dynamic coupling.

SUMMARY/CONCLUSIONS

The analysis described in this article confirms that *true* multiaxis vibration simulation is possible within the constraints of existing hardware. Much of the results presented here have been recognized qualitatively for some time, but have never been addressed from a quantitative perspective: this is the contribution of this study. The issue of kinematic constraints was addressed for both fixed and variable LOA force inputs. It was shown that fixed LOA force inputs require movable actuator attachment points; variable LOA force inputs require additional constraints (in particular, the x and y translations of the c.m. in $\mathcal{F}_B$ and the rotation about the yaw axis). It was also shown that by using six variable LOA force inputs, 6-DOF simulation is possible without additional constraints; however, special measures are needed to compensate for the kinematic and dynamic coupling that occurs in the system. A mechanism for determining the required actuator commands for both 3- and 6-DOF simulation was also presented.

The analysis presented here has direct implications on the development of closed-loop control systems for multiaxis simulation.

The author wishes to thank Mr. Oscar Estrada and Mr. Mike Hale of the RTTC Dynamic Test Branch for their helpful suggestions and discussions.

REFERENCES

Fitcher, E. F., 1986, "A Stewart Platform-Based Manipulator: General Theory and Practical Considerations," *The International Journal of Robotics Research,* Vol. 5, pp. 157–182.

Fitz–Coy, N. G., and Chatterjee, A., 1994, "Actuator

Placement in Multi-Degree-of-Freedom Vibration Simulators," *Shock and Vibration,* Vol. 1, pp. 279–288.

Goldstein, H., 1980, *Classical Mechanics,* 2nd ed., Addison–Wesley Publishing Co., Reading, MA.

Golub, G. H., and Van Loan, C. F., 1989, *Matrix Computations,* 2nd ed., Johns Hopkins University Press, Baltimore, MD.

Hahn, H., and Raasch, W., 1986, "Multi-Axis Vibration Test on Spacecraft Using Hydraulic Exciters," in *AGARD Mechanical Qualification of Large Space Structures,* pp. 23.1–23.23.

Hunt, K. H., 1978, *Kinematic Geometry of Mechanisms,* Oxford University Press, Oxford, UK.

Merklinghaus, W., 1977, "Computer Controlled Hydraulic Earthquake Simulation for Testing H.V. Switch Gear," *Siemens Review,* Vol. XLIV.

Stewart, D., 1965, "A Platform with Six Degrees of Freedom," *Proceedings of the Institute of Mechanical Engineering,* Vol. 180, pp. 371–386.